Eur. Phys. J. E **24**, 145–156 (2007)
DOI 10.1140/epje/i2007-10225-1

THE EUROPEAN PHYSICAL JOURNAL E

Magneto-vibratory separation of glass and bronze granular mixtures immersed in a paramagnetic liquid

P. López-Alcaraz, A.T. Catherall, R.J.A. Hill, M.C. Leaper, Michael R. Swift, and P.J. King[a]

School of Physics and Astronomy, University of Nottingham, Nottingham, NG7 2RD, UK

Received 4 April 2007 and Received in final form 18 July 2007
Published online: 31 October 2007 –

Abstract. A fluid-immersed granular mixture may spontaneously separate when subjected to vertical vibration, separation occurring when the ratio of particle inertia to fluid drag is sufficiently different between the component species of the mixture. Here, we describe how fluid-driven separation is influenced by magneto-Archimedes buoyancy, the additional buoyancy force experienced by a body immersed in a paramagnetic fluid when a strong inhomogeneous magnetic field is applied. In our experiments glass and bronze mixtures immersed in paramagnetic aqueous solutions of $MnCl_2$ have been subjected to sinusoidal vertical vibration. In the absence of a magnetic field the separation is similar to that observed when the interstitial fluid is water. However, at modest applied magnetic fields, magneto-Archimedes buoyancy may balance the inertia/fluid-drag separation mechanism, or it may dominate the separation process. We identify the vibratory and magnetic conditions for four granular configurations, each having distinctive granular convection. Abrupt transitions between these states occur at well-defined values of the magnetic and vibrational parameters. In order to gain insight into the dynamics of the separation process we use computer simulations based on solutions of the Navier-Stokes' equations. The simulations reproduce the experimental results revealing the important role of convection and gap formation in the stability of the different states.

PACS. 45.70.Mg Granular flow: mixing, segregation and stratification

1 Introduction

Granular materials are widespread both in nature and in commerce. In many industrial applications it is very important to be able to separate granular materials, obtained, for example, from mined ores, into their constituent components. A number of important separation techniques have been successfully based on differences in size, density or roughness [1,2]. However, when grains move within a fluid, and the grains are fine enough for the fluid-grain interactions to be strong, it is generally the fluid-grain interactions which dominate the dynamics, and therefore the separation processes.

This paper concerns the influence of magnetic buoyancy on the fluid-driven separation of fine granular mixtures under low-frequency vibration.

In the absence of magnetic forces a granular mixture subjected to vertical vibration in the presence of a fluid may spontaneously separate [3,4]. Grains are thrown from a platform undergoing sinusoidal vertical motion $z_p = A\sin(\omega t)$ if the dimensionless acceleration of the platform $\Gamma = A\omega^2/g$ exceeds unity. Here A is the amplitude of vibration, g is Earth's gravity and $\omega = 2\pi f$ is the angular frequency of vibration. While the grains move upwards after being thrown, fluid is drawn down through the bed to fill the space below. Later in the vibration cycle, when the grains fall back towards the platform, fluid is forced up through the bed. It is this periodic fluid flow which leads to separation if the ratio of particle inertia to fluid-drag force is sufficiently different between the species of the mixture [3,4]. Here, we refer to this as the vibratory inertia/fluid-drag (VIFD) mechanism. However, if the fluid is paramagnetic it will be drawn towards the strongest part of any magnetic field in which it is placed. The grains will then be subjected to magnetic buoyancy forces which may act to reinforce or to counteract VIFD separation. It is the influence of this magneto-Archimedean buoyancy on VIFD separation which we report here.

In the case of a fluid of negligible density, such as air, and in the absence of a magnetic field, VIFD separation will occur if the granular components have distinctly different ratios of inertial mass to fluid drag. At low Reynolds' numbers, such that the flow is laminar, the drag forces per particle scale as ηd, where d is the particle diameter and η is the dynamic viscosity of the fluid. That constituent of the mixture having the greater ratio of inertia mass to fluid drag will then present a larger value of $\rho d^2/\eta$. Here ρ is the density of the granular material. In isolation a group of these grains thrown by vibration

[a] e-mail: p.j.king@nottingham.ac.uk

will tend to fly higher than an isolated group of grains having a lower value of $\rho d^2/\eta$. A detailed analytical treatment of the conditions for the separation of a mixed bed is not available. However, it might be supposed that over many cycles of vibration the mixture will separate with the grains of higher $\rho d^2/\eta$ in the upper part of the granular bed. Detailed studies of the fluid-driven separation of fine bronze and glass granular mixtures vibrated in air have shown that, at low frequencies, this is indeed the case [3,4], and that the VIFD separation of a mixture consisting of grains of type a and b may be predicted by examining the parameter $S = \rho_a d_a^2/\rho_b d_b^2$. At low frequencies grains of type a will separate above grains of type b if S is appreciably greater than unity. The separation may be essentially complete, the boundary between the separated layers being sharp and well defined [3,4].

The complexity of the problem is illustrated by noting that at sufficiently high frequencies separation still occurs if S is appreciably different from unity, but that the higher ρd^2 component is then found sandwiched between an upper and a lower region of the lower ρd^2 component [3,4]. At high frequencies, periodic spatial oscillations are found at high values of Γ. These effects have not yet been fully explained despite extensive computer simulation [5].

For grains in a liquid, an analysis of the conditions for VIFD separation is further complicated by the appreciable fluid density. This results in buoyancy forces, mass correction effects and Basset history forces [6], each of which influence the granular dynamics. The mass corrections and history forces are known for an isolated spherical particle moving within a dense fluid [7,8] but the expressions for such forces on a particle moving within a dense granular bed are unknown. Nevertheless, in studies of VIFD separation of water-immersed binary mixtures, the parameter S is still useful in approximately determining the condition for separation [9]. At low frequencies an appreciably higher ρd^2 component is found above the lower ρd^2 component.

At low frequencies of vibration, a granular bed is unstable against the development of Faraday tilting [10,11]. Should any tilt of the upper surface occur, horizontal components of the fluid flow will enhance the tilt until a dynamic angle of repose is reached. The resulting fluid-driven granular convection speeds the separation process [12]. During the development of VIFD separation, like grains will interact similarly with the fluid and will stay together; grains of different ρd^2 will be drawn apart. Groups of the two species coarsen, the process usually leading to a single region of each type. Since they have distinct values of ρd^2, these regions will be thrown with distinct flight paths, gaps opening between them during flight. It is found that convective motion principally occurs while these gaps are open, enabling convective motion within each region without the two regions mixing [9].

Catherall *et al.* have shown that fine granular mixtures vibrated in vacuum may be effectively separated through the use of a strong and inhomogeneous magnetic field if the component grains have sufficiently distinct magnetic susceptibilities [13]. It is well known that a paramagnetic or diamagnetic body of volume V in the presence of a vertically inhomogeneous magnetic field B will experience a vertical force F given by

$$F = \frac{\chi V}{\mu_0} B \frac{\mathrm{d}B}{\mathrm{d}z}\,, \tag{1}$$

where χ is the magnetic susceptibility of the body and μ_0 is the magnetic permeability of vacuum [14]. The body behaves as if it is exposed to an effective gravitational force $\rho V \tilde{g}$ where

$$\tilde{g} = g - \frac{\chi}{\rho\mu_0} B \frac{\mathrm{d}B}{\mathrm{d}z}. \tag{2}$$

When $\tilde{g} = 0$, a diamagnetic object may achieve magnetic levitation [15–17]. Diamagnetic levitation was initially proposed by Lord Kelvin, firstly observed by Braunbeck [15,16] and famously demonstrated by Berry and Geim [17]. In magnetic fields insufficient to cause complete levitation, those components of a vibrated granular mixture which have a lower $\tilde{g}$ will tend to be thrown higher than those having a larger $\tilde{g}$, and over many cycles the mixture will separate. In experiments on bismuth-bronze mixtures the degree of separation has been found to be a continuous function of the magnetic and vibrational parameters [13].

When similar experiments are conducted in air, the magnetic separation mechanism may act in concert with the VIFD separation mechanism or may oppose it. The two may cancel leading to mixing. As a result a number of distinct mixed and separated states are found each with its own distinctive convection. The system changes abruptly between these states as the control parameters are adjusted [18,19].

A related magnetic separation mechanism, that discussed here, occurs when a granular mixture is vibrated inside a paramagnetic fluid held within an inhomogeneous magnetic field. A paramagnetic fluid experiences a force moving it towards stronger fields, leading to a magneto-Archimedes buoyancy force on any objects within the fluid. This magnetic buoyancy acts in concert with Earth's gravitational force and with normal Archimedean buoyancy. If only static forces are considered, the body may then be considered to experience an effective gravity given by

$$\tilde{g} = g - g\frac{\rho_f}{\rho} - \frac{(\chi - \chi_f)}{\rho\mu_0} B \frac{\mathrm{d}B}{\mathrm{d}z}\,, \tag{3}$$

where ρ_f and χ_f are the density and susceptibility of the surrounding fluid. In the above expression the term proportional to χ_f represents the magneto-Archimedes buoyancy force. Since a paramagnetic fluid may be far more strongly magnetic than diamagnetic granular materials, using such a fluid enables the use of smaller $|B\mathrm{d}B/\mathrm{d}z|$ to achieve levitation or magneto-vibratory separation [20–23]. Note that if the paramagnetic susceptibility of the fluid dominates the magnetic properties of the grains themselves, the magnetic separation mechanism will be based on differences in the particle density, while the VIFD separation which we have described above is based on differences in the product ρd^2. If negative values

of $B\mathrm{d}B/\mathrm{d}z$ are applied, as in the present work, lighter grains experience a lower $\tilde{g}$ and for sufficient magnitudes of $|B\mathrm{d}B/\mathrm{d}z|$ will be expected to separate to the top of the bed, while under fluid-driven vibratory separation alone they would tend to separate to the bottom of the bed. If positive values of $B\mathrm{d}B/\mathrm{d}z$ are applied the two separation mechanisms are expected to act in concert.

Here, we describe how magneto-Archimedean buoyancy forces influence the VIFD separation of bronze and glass granular mixtures subjected to vertical sinusoidal vibration. The paramagnetic fluids used are aqueous solutions of $MnCl_2$ of different molar concentrations. In the absence of any magnetic force, the granular mixtures separate under vertical vibration approximately according to their S ratios, since only the VIFD separation mechanism is present. However, in the presence of an inhomogeneous magnetic field and vibration a granular mixture adopts a number of distinct mixed and separated states which may be selected by choosing the magnetic and vibratory conditions. Insight into the dynamics of the separation is achieved through computer simulations in which the fluid movement is treated through the Navier-Stokes' equations. These simulations enable us to clarify details of the separation behaviour which are very difficult to investigate through experimentation.

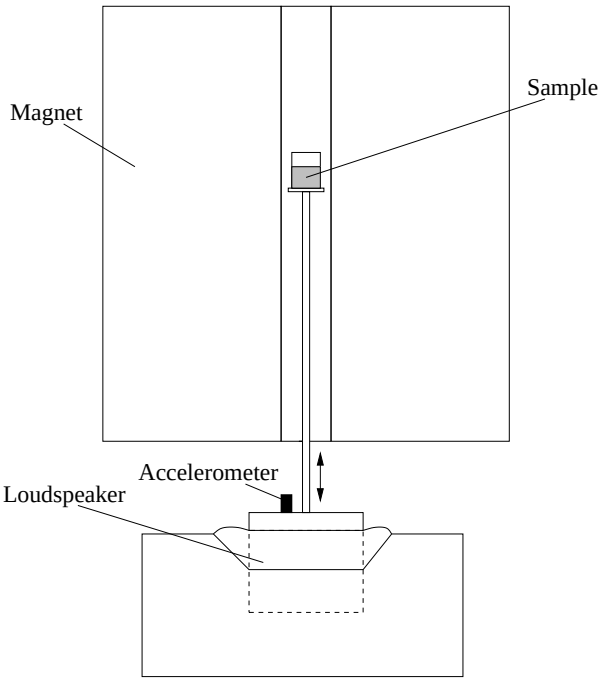

Fig. 1. Schematic diagram of the apparatus showing the granular sample positioned within the vertical magnet bore, and the method of vibration.

2 Experimental details

The magnetic fields used in these experiments were generated by an Oxford Instruments superconducting magnet with a closed-cycle cooling system. The magnet has a vertical open bore of 5 cm diameter and produces a maximum field of 17 T and a maximum $B\mathrm{d}B/\mathrm{d}z$ of $\pm 1470\,\mathrm{T^2 m^{-1}}$. The value of $B\mathrm{d}B/\mathrm{d}z$ can be controlled by varying the current in the superconducting coils. In these experiments the granular mixtures were positioned in the upper part of the magnet bore in the region where $B\mathrm{d}B/\mathrm{d}z$ is maximally negative.

A granular sample under investigation was held in a soda-glass box of horizontal dimensions 10 mm by 40 mm and of height 40 mm. The mean depth of a granular mixture was always close to 20 mm when at rest. Due to the dimensions of the box, the mean motion of the grains during vertical vibration is observed to be confined to the plane defined by the two larger dimensions of the box [9]. The grains of all our mixtures were given a $\pm 10\%$ size distribution in order to prevent crystallisation effects during vibration. The experimental arrangement is shown in Figure 1. The soda-glass box was mounted on a 48 mm circular plinth, which was bolted to the top of a thin-walled stainless-steel rod. The rod passed down through the open bore of the magnet and a slide bearing, not shown in the figure. The bottom of the rod is bolted to a long-throw loudspeaker [13]. A cantilever capacitance accelerometer attached to the bottom of the rod was used to measure the amplitude of vibration. In the region within the bore of the magnet occupied by the grains during vibration, the product $B\mathrm{d}B/\mathrm{d}z$ varies by less than 5%. Small radial forces are also present for off-axis grains. However, these forces are less than 5% of the vertical force in magnitude and are considered negligible in our experiments. Further details of the experimental apparatus and of the magnetic field profiles may be found in references [13] and [24].

Before vibration, a particular $MnCl_2$ aqueous solution was poured in the soda-glass box which contained the granular mixture under investigation. Then the soda-glass box was shaken to remove any air bubbles trapped within the grains. Once free of bubbles, the grains were stirred with a spatula in order to achieve a near-homogeneous mixture. The granular mixtures consisted of spherical soda-glass grains sourced from Potters Ballotini Ltd. and spherical bronze grains sourced from Makin Powders Ltd. The density of the glass grains used is $2500 \pm 25\,\mathrm{kg\,m^{-3}}$, while that of the bronze grains is $8900 \pm 25\,\mathrm{kg\,m^{-3}}$. In our experiments, 50% : 50% mixtures by volume were used throughout. The magnetic susceptibility of both components is approximately -5×10^{-6}. These susceptibilities may be considered negligible when compared to those of the paramagnetic fluids used in these experiments. The temperature in the bore of the magnet was kept at 20 °C. In all the experiments the vibrational frequency was fixed at 20 Hz, the separation being studied as a function of Γ and the $B\mathrm{d}B/\mathrm{d}z$ applied.

3 Initial results

We first describe the behaviour of a glass and bronze mixture with both components having a mean particle diameter of 1090 μm. The S parameter of this mixture is about 3.6. Thus, if vibrated in water, the denser bronze

grains would separate on top of the glass grains [9]. The mixture was immersed in a $MnCl_2$ aqueous solution with a molar concentration of 1.5 M. The density, dynamic viscosity and magnetic susceptibility of this solution are respectively $\rho_f = 1145\,\mathrm{kg\,m^{-3}}$, $\eta = 1.6 \times 10^{-3}\,\mathrm{Pa\,s}$ and $\chi_f = 260 \times 10^{-6}$. The vibrational frequency was fixed at 20 Hz whilst $\Gamma = 2.0$. With the vibrational parameters fixed, only $B\mathrm{d}B/\mathrm{d}z$ was varied. At the frequency used, Faraday tilting and its associated fluid-driven convection are clearly evident.

When no magnetic force is applied, the separation is dominated by the VIFD mechanism and the mixture behaves similarly to its behaviour if immersed in water. At the vibratory conditions applied, the denser bronze grains accumulate on top of the bed. The sequence of the separation can be observed in Figure 2(a). By about 30 s after vibration starts, the bed has broken symmetry through Faraday tilting. As the bed starts to tilt, the denser bronze grains accumulate in the upper regions of the bed. At the same time the bed acquires the granular convection indicated by the overlaid arrowed white lines. By approximately 50 s almost all of the bronze particles are on top of the glass grains. Two well-defined convection cells may be observed, one in the upper bronze layer and the other in the lower glass region. Despite apparent opposite granular flow at the boundary between the layers, the boundary remains sharp. These observations are in agreement with the previous observations by Leaper *et al.* on VIFD separation in water [9].

The application of an inhomogeneous magnetic field can completely change the separation behaviour. For the $MnCl_2$ solution used here the $\tilde{g}$ of the glass grains becomes zero when a $B\mathrm{d}B/\mathrm{d}z$ of approximately $-63\,\mathrm{T^2m^{-1}}$ is applied. However, a magnetic force just half of that required to levitate the glass is sufficient to completely modify the segregation of the mixture under investigation. Figure 2(b) shows the separation process when a $B\mathrm{d}B/\mathrm{d}z$ of $-30\,\mathrm{T^2m^{-1}}$ is applied. Under this $B\mathrm{d}B/\mathrm{d}z$, the $\tilde{g}$ of glass is reduced to $2.7\,\mathrm{m\,s^{-2}}$, whilst $\tilde{g}$ for bronze is $7.8\,\mathrm{m\,s^{-2}}$. This difference is sufficient to counteract the tendency to form VIFD separation through differences of density noted for zero field and, in equilibrium, the components remain partially mixed and the bed displays a single convection cell. However, for a $B\mathrm{d}B/\mathrm{d}z$ of $-50\,\mathrm{T^2m^{-1}}$, the separation process is completely inverted, as may be observed in Figure 2(c). With this magnetic force, $\tilde{g} = 1.0\,\mathrm{m\,s^{-2}}$ for the glass grains and $7.3\,\mathrm{m\,s^{-2}}$ for the bronze grains. Thanks to their small effective gravity the glass grains quickly migrate to the top during vibration, accumulating on top of the bronze particles. After a few cycles of vibration, a pure glass bed is found above a pure bronze bed with a sharp boundary existing between them. If a $B\mathrm{d}B/\mathrm{d}z$ of $-45\,\mathrm{T^2m^{-1}}$ with $\Gamma = 3.5$ is applied, a fourth type of separation is observed, that shown in Figure 2(d). Here bronze grains are sandwiched between a lower and an upper region of glass grains. These initial results clearly illustrate how the differences in effective gravities generated by the magneto-Archimedes buoyancy can effectively modify the VIFD separation process.

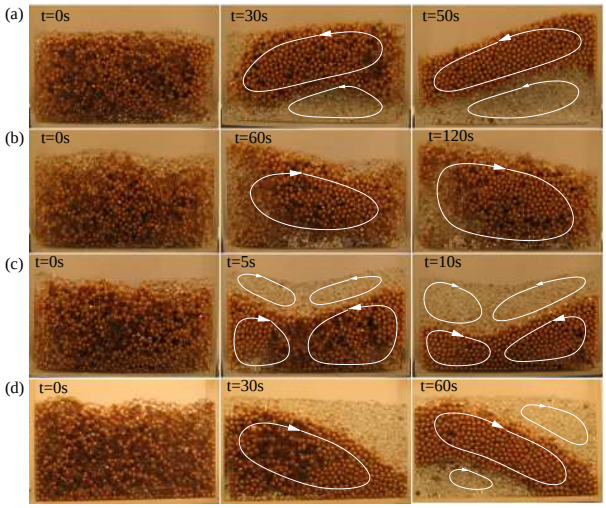

Fig. 2. Sequences of the segregation process of glass and bronze grains of mean diameter 1090 μm from the initially well-mixed state to the equilibrium state. The grains were vibrated at 20 Hz in a 1.5 M aqueous solution of $MnCl_2$ using different values of $B\mathrm{d}B/\mathrm{d}z$ and Γ: (a) $0\,\mathrm{T^2m^{-1}}$ and $\Gamma = 2.0$; (b) $-30\,\mathrm{T^2m^{-1}}$ and $\Gamma = 2.0$; (c) $-50\,\mathrm{T^2m^{-1}}$ and $\Gamma = 2.0$; (d) $-45\,\mathrm{T^2m^{-1}}$ and $\Gamma = 3.5$. The thicker arrowed lines represent faster convective flow completing one loop in typically 10–20 s. The thinner lines indicate convective flows typically 10 times slower than this.

4 Detailed observations

The effect of varying the values of Γ and $B\mathrm{d}B/\mathrm{d}z$ on the separation behaviour has been investigated in detail for a number of mixtures at the fixed vibrational frequency of 20 Hz. In each case Γ was varied between 1 and 6 and the $B\mathrm{d}B/\mathrm{d}z$ applied was varied between zero and a value just less than that required to fully levitate the glass grains.

The system with 1090 μm diameter bronze and glass grains immersed in a 1.5 M $MnCl_2$ solution was the first to be analysed in more detail. Depending upon the values of Γ and $B\mathrm{d}B/\mathrm{d}z$, the mixture was observed to adopt one of the four equilibrium states described above. We name these states *bronze on top*, *partially mixed*, *glass on top* and *sandwich*. Figures 2(a), (b), and (c) respectively represent examples of the first three states. Figure 2(d) represents an example of the *sandwich* state. In previous works on the separation of water-immersed glass and bronze mixtures, the *sandwich* configuration has been observed to be a metastable state which eventually evolves into a *bronze-on-top* state [9]. However, in our experiments, we observe that once such state is achieved, it remains unmodified in time over the periods investigated, several hours.

The schematic diagram exhibiting the vibratory and magnetic conditions needed to achieve the different equilibrium states is shown in Figure 3. The mixture was always vibrated from an initially well-mixed initial configuration. Although for this mixture the timescale to achieve the equilibrium state is typically 1–2 minutes, some of the experiments were left running for far longer periods in order to confirm the stability of each of the equilibrium

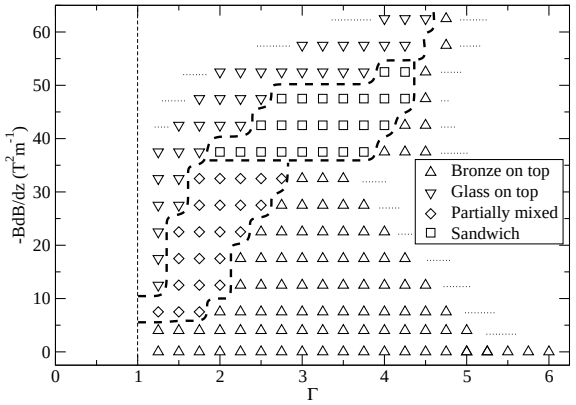

Fig. 3. Schematic diagram of the different equilibrium states of a glass and bronze mixture of mean diameter 1090 μm as a function of $B\mathrm{d}B/\mathrm{d}z$ and Γ when immersed in a 1.5 M $MnCl_2$ solution. The vibrational frequency was 20 Hz. The approximate boundaries between the different equilibrium configurations are shown by the broken lines.

states. In the diagram, clear regions corresponding to the *bronze-on-top*, *partially mixed*, *sandwich* and *glass-on-top* states are evident. Each equilibrium state is associated with a distinct pattern of convection cells and the change in the behaviour at the boundaries between the different regions is abrupt. The uncertainty in determining these boundaries is typically $\pm 5\%$ in $B\mathrm{d}B/\mathrm{d}z$ and ± 0.1 in Γ. The positions of these boundaries are roughly indicated by broken lines as a guide to the eye. In additional experiments we have observed that the final state reached by the mixture was independent of the initial configuration of the grains. The same final state results whether the initial condition is a homogeneously mixed state or is one of the other configurations. This is true for all the experiments reported here. In examining this diagram it is to be noted that at low values of $B\mathrm{d}B/\mathrm{d}z$, and particularly at higher values of Γ, the *bronze-on-top* state is found. At high magnetic fields and particularly at lower values of Γ, the *glass-on-top* state is found. The *partially mixed* and *sandwich* states are found in the boundary region between these two extremes, a region extending from the bottom left to the top right of the diagram, that is from low fields and low Γ to high fields and high Γ.

To study the influence of the magnetic fluid, the experiments were repeated using $MnCl_2$ solutions having molar concentrations of 0.5 M, 1.0 M, 2.25 M and 3.0 M. Their properties are summarised in Table 1. In each case bronze and glass grain sizes of 1090 μm and a frequency of 20 Hz have been used. For each magnetic fluid, the four equilibrium states which we have described above are found and in very similar topological arrangements within the ($B\mathrm{d}B/\mathrm{d}z$, Γ)-plane.

In such complex systems it is not surprising that no simple criterion has been developed for predicting the values of Γ and $B\mathrm{d}B/\mathrm{d}z$ for which the four equilibrium states occur. Certainly we are not aware of any generalisation of the parameter S to include magnetic forces. However, in analysing these results qualitatively, a number of important features may be understood by noting that the dynamics principally result from the interplay of the inertia of the particles, proportional to their volume and density, the dominant magnetic buoyancy forces proportional to $V\chi_f B\mathrm{d}B/\mathrm{d}z$, and the fluid-drag forces. At the low Reynolds number used here, the latter are proportional to the product of ηd and the relative velocity of the fluid and the grains. For equal-sized bronze and glass mixtures, such as those used to obtain Figure 3 and at low magnetic fields, the interplay between inertia and fluid drag leads to VIFD separation with the bronze uppermost At high magnetic fields magnetic buoyancy dominates the fluid drag and the most buoyant material, glass, is found uppermost. The fluid-drag term is proportional to the relative velocity of the liquid and the grains. This relative velocity will increase approximately linearly with Γ. Thus, as Γ is increased, larger values of the magnetic field will be needed to dominate fluid drag and therefore to pass from the *bronze-on-top* state to the *glass-on-top* state. This is just the trend shown in Figure 3. These general arguments are not sufficient, however, to explain the presence and the extent of the *partially mixed* and *sandwich* states found along the border.

Table 1. Measured properties of the $MnCl_2$ solutions used. The dynamic viscosity of distilled water at 20 °C is equal to $\eta_0 = 1 \times 10^{-3}$ Pa s.

Molar concentration (M)	ρ_f (kg m^{-3})	η/η_0	χ_f ($\times 10^{-6}$)
0.50	1050	1.1	85
1.00	1090	1.3	170
1.50	1145	1.6	260
2.25	1220	2.0	370
3.00	1290	2.6	485

We further note that the magnetic forces are always of the form $V\chi_f B\mathrm{d}B/\mathrm{d}z$. The principal effect of changing the molar concentration of the manganese chloride solution is to change the susceptibility, with smaller changes in the viscosity and density. It is therefore to be expected that the equilibrium state diagrams, of which Figure 3 is an example, will be very similar in form but for a change in scale along the vertical $B\mathrm{d}B/\mathrm{d}z$ axis. To test this supposition we have measured the value of the $B\mathrm{d}B/\mathrm{d}z$ threshold necessary to achieve the *glass on top* as a function of the susceptibility of the $MnCl_2$ solutions. To minimise the effect of fluid-driven convection, the measurements were carried out at $\Gamma = 1.25$. The results can be seen in Figure 4, in which the data is plotted as $\chi_f B\mathrm{d}B/\mathrm{d}z$ against χ_f. It may be seen that, as is expected, $\chi_f B\mathrm{d}B/\mathrm{d}z$ does not depend strongly upon χ_f. The slight reduction with increasing χ_f must be attributed to the increases in viscosity and fluid density with increasing $MnCl_2$ molar fraction. The boundary which we are examining is principally determined by the interplay of magnetic and drag forces

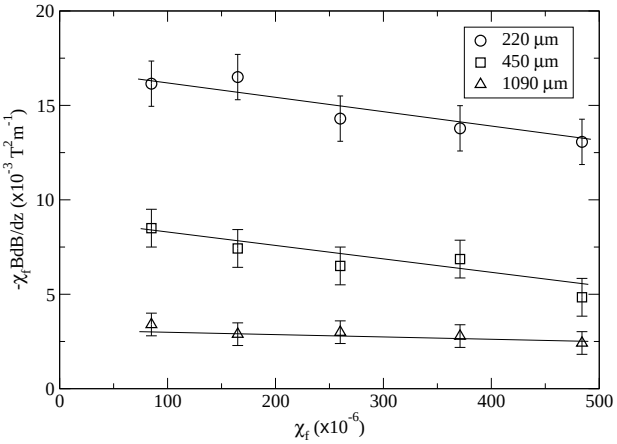

Fig. 4. Value of the $-\chi_f B\mathrm{d}B/\mathrm{d}z$ threshold needed to achieve the *glass-on-top* configuration at 20 Hz and $\Gamma = 1.25$ as a function of the susceptibility of the magnetic solution, χ_f. Data are shown for three glass and bronze mixtures of mean diameters 1090 μm ($\triangle$), 450 μm ($\diamond$), 220 μm ($\circ$).

which we again note are proportional to the product of ηd and the relative velocity of the fluid and the grains. The viscosity is substantially increased by going from 0.5 M to 3 M $MnCl_2$ solutions, but the effect of this increase is to damp the motion of the bed, substantially reducing the relative velocity of the fluid and the grains. Numerical simulations, the details of which we shall present below, show that the effect on the fluid drag of changing the viscosity is far smaller than the change in viscosity itself, as is evident from Figure 4.

To study the influence of particle size while keeping the mean size of the two components equal, the experiments described above were repeated using two mixtures of mean size 450 μm and 220 μm, respectively. The S parameter for each mixture is also 3.6. Thus, when no magnetic force is applied the grains separate into the *bronze-on-top* configuration. In a magnetic field the four equilibrium states described above were found for each grain size. Again the $B\mathrm{d}B/\mathrm{d}z$ threshold needed to achieve the *glass on top* was studied. The results are shown in Figure 4. It may be seen that for each grain size the threshold values of $\chi_f B\mathrm{d}B/\mathrm{d}z$ are not a strong function of χ_f, but that the threshold values increase substantially with a reduction in particle size.

We may qualitatively understand this dependence on particle size as follows. As the mean particle size is reduced, the influence of fluid damping increases. Therefore, stronger magnetic forces are necessary to completely counteract the separation tendencies of the fluid-drag mechanism. However, the magnetic force is proportional to $V\chi_f B\mathrm{d}B/\mathrm{d}z$ and therefore to $d^3\chi_f B\mathrm{d}B/\mathrm{d}z$. If we suppose laminar flow, then the fluid-drag forces are proportional to the mean particle size d. If we assume that the *glass-on-top* state is achieved when the magnetic forces overcome the drag interactions, we should expect $\chi_f B\mathrm{d}B/\mathrm{d}z$ to be proportional at the boundary to $1/d^2$. However, were we to suppose non-linear flow such that the second term of the Ergun equation dominates [25], then the fluid-drag forces would be proportional to d^2. We should then expect $\chi_f B\mathrm{d}B/\mathrm{d}z$ to be proportional at the boundary to $1/d$, The Reynolds number corresponding to $\Gamma = 1.25$ is about 3, suggesting that the fluid behaviour is closer to the laminar than the fully non-linear regime. However, the increased damping caused by a reduction in the magnitude of d will lead to a reduction in the relative velocities of the fluid and grains, partially compensating for the change in d. Thus we should expect $\chi_f B\mathrm{d}B/\mathrm{d}z$ to be proportional at the boundary to $1/d^n$, where n is appreciably less than 2. The data of Figure 4 display a dependence corresponding to $n = 1.1 \pm 0.1$.

4.1 Varying the particle size ratio

We have also investigated the effects of varying the size ratio of the glass and bronze grains. Initially, we consider glass and bronze mixtures in which the mean size of bronze grains is kept constant and equal to 1090 μm, while the mean size of the glass grains is reduced. The glass grains used were of mean sizes 900, 780, 550, 350 and 160 μm, each with a spread of sizes of $\pm 10\%$. These provide mixtures with S ratios of 5.2, 6.9, 14, 34 and 165, respectively. All the mixtures were vibrated while immersed in the 1.5 M solution. The smaller the mean diameter of the glass grains in the mixtures, the higher the S parameter and, consequently, the higher the influence of fluid-drag forces on the motion of the glass particles. It is expected, therefore, that stronger magnetic forces will be needed to completely overcome the VIFD separation mechanism. That this is so is clear if Fig. 3 is compared with Figure 5, which shows the vibratory and magnetic conditions necessary to obtain the different equilibrium configurations for the mixture of $S = 14$. Here, most of the diagram is dominated by the *bronze-on-top* state. Only when the $B\mathrm{d}B/\mathrm{d}z$ applied is approximately $-52\,\mathrm{T^2m^{-1}}$ can the differential gravity separation mechanism overcome the VIFD mechanism so that the mixture can be separated with the *glass on top*. Topologically similar diagrams were found for the rest of the mixtures described above. For the mixtures of the S parameter 5.2 and 6.9, the value of the $B\mathrm{d}B/\mathrm{d}z$ threshold necessary to achieve the *glass-on-top* configuration is found to be approximately of the form $B\mathrm{d}B/\mathrm{d}z \propto 1/d^n$, where n is somewhat less than 2. Here d represents the mean diameter of the glass grains. This dependence is consistent with the relationship described in the previous section if the large grains dominate the mean grain-fluid velocity. However, as the size of the glass grains was further reduced, the threshold value for the *glass-on-top* configuration was found to tend asymptotically towards $-60\,\mathrm{T^2m^{-1}}$, a value close to the one required for the full magneto-Archimedes levitation of the glass grains. If the glass grains are small enough, size segregation effects may play a role. Then, the arguments used to justify the $1/d^2$-dependence are no longer appropriate.

Finally we have repeated the experiments described above using a mixture in which the mean size of the glass grains was 1090 μm, while the mean size of the bronze particles was 550 μm. These sizes have been selected so

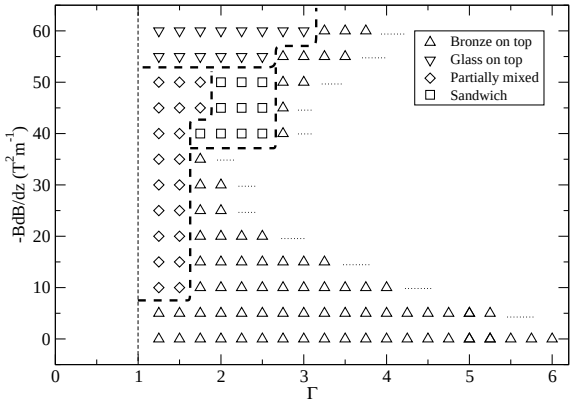

Fig. 5. Schematic diagram showing the different equilibrium states of a mixture of 550 μm glass and 1090 μm bronze as a function of $B\mathrm{d}B/\mathrm{d}z$ and Γ when immersed in a 1.5 M $MnCl_2$ solution. The broken lines offer, as a guide to the eye, the approximate boundaries between the different equilibrium configurations. The frequency of vibration was 20 Hz.

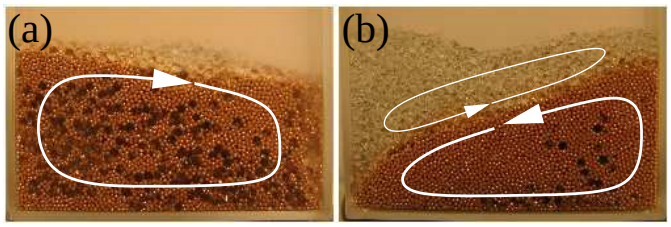

Fig. 6. Image showing the two equilibrium configurations which can be obtained when a mixture with of 1090 μm glass and 550 μm bronze immersed in a 1.5 M $MnCl_2$ aqueous solution is vertically vibrated with: (a) $\Gamma = 3.5$ and zero magnetic field; (b) $\Gamma = 3.5$ and $B\mathrm{d}B/\mathrm{d}z = -40\,\mathrm{T^2m^{-1}}$. The frequency of vibration was 20 Hz.

that the S parameter is close to unity. No VIFD separation is expected and indeed under vibration the mixture maintains a mixed state in the absence of magnetic fields. Depending on the magnetic field applied, this mixture is found to have two equilibrium states, a low-field *partially mixed* state and a higher-field *glass-on-top* state. An example of both states is shown in Figure 6. Figure 7 shows, schematically, the vibratory and magnetic conditions needed to achieve these two equilibrium states. If Figures 3, 5 and 7 are compared, it can clearly be noted how the region corresponding to the *glass-on-top* state diminishes as the S parameter of the mixture increases.

From Figures 2 and 7 it can easily be observed that whenever a mixture separates into a number of distinct layers, whether it is a *bronze-on-top*, a *glass-on-top* or a *sandwich* configuration, the boundary between the layers remains sharp despite opposite granular flow at the boundaries. This is due to the formation of spatial gaps between the separated layers during flight [4,9]. Importantly, the convective motion takes place while these gaps are open. We have confirmed the presence of these gaps using computer simulations.

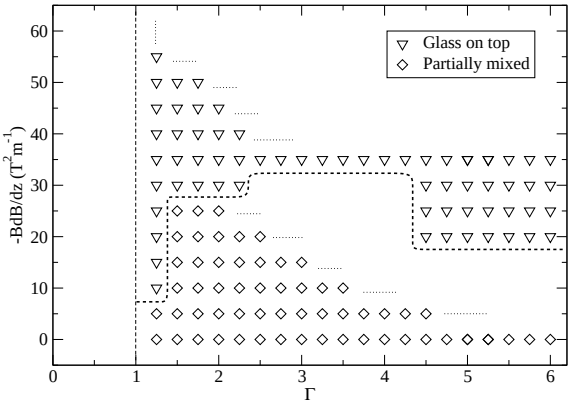

Fig. 7. Schematic diagram showing the different equilibrium states of a mixture of 1090 μm glass and 550 μm bronze as a function of $B\mathrm{d}B/\mathrm{d}z$ and Γ when immersed in a 1.5 M $MnCl_2$ solution. The broken lines represent the approximate boundaries between the different equilibrium configuration. The frequency of vibration was 20 Hz.

We have also carried out experiments on a range of different container widths. For wider containers separation states are found as we have described and separation is rapid. For very narrow boxes, however, granular convection is suppressed and the times for separation become very long. The sandwich state is found over a wider range of $B\mathrm{d}B/\mathrm{d}z$ and Γ than for boxes where convection is evident, but it may well be a long-lived metastable state.

5 Simulation techniques

We have noted that an analytical treatment of the separation process is not available and that while general arguments based on considering the forces acting on the particles are sufficient to determine some principal features, many behaviours cannot be simply predicted in this way. We therefore resort to numerical simulation to aid our understanding. These computer simulations are not an attempt to accurately reproduce all the details of our experiments, which would be rather difficult with the computational power we can access, but are used to help us identify the key features of the separation dynamics.

In these simulations, the grains are considered to be perfect spheres having a spread of diameters of $\pm 10\%$ about the mean, which interact with each other and with the container walls via inelastic collisions. Particle rotation is not considered. The collisions are treated using the linear spring-dashpot model in the normal direction and using simple Coulomb friction in the tangential direction [26]. The dashpot damping is adjusted to correspond to the normal coefficient of restitution required. Within a liquid the restitution coefficient is expected to be very low for low Stokes' numbers [27]. We have examined a range of values of normal restitution and find that the results are not sensitive to its value provided it is set substantially

Table 2. Particle and fluid parameters used in the simulations.

Parameter	Value
Particles diameter	900–1100 μm
Density of bronze	8900 kg m^{-3}
Density of glass	2500 kg m^{-3}
Magnetic susceptibility of bronze	-5×10^{-6}
Magnetic susceptibility of glass	-5×10^{-6}
Fluid Susceptibility	260×10^{-6}
Container dimensions (mm)	$40 \times 4 \times 40$
Spring constant	3000 N m^{-1}
Coefficient of restitution	0.1–0.9
Particle friction coefficient	0.2
Wall friction coefficient	0.2
Fluid density	1150 kg m^{-3}
Fluid dynamic viscosity	1.5×10^{-3} Pa s

less than unity. Most of the simulations have been carried out with a value of 0.1. Gravitational forces, and conventional and magnetic Archimedean buoyancy forces in a form appropriate to the accelerating frame of reference of the container, are applied directly to the grains. The equation of motion of each grain is solved using a second-order time-stepping Verlet algorithm [28]. The simulation parameters used are shown in Table 2. The vertical and one of the horizontal dimensions of the simulated container were equal to those of the experimental box. However, to speed computation one of the horizontal dimensions was reduced to 4 mm since the motion of the grains in our experimental systems is almost two-dimensional, the dimensions along which the granular motion takes places being those of the larger faces of the box. The simulated fluid is given the same characteristics as the 1.5 M $MnCl_2$ aqueous solution and is considered to be incompressible [29]. We note that while grain-wall friction drives the granular convection in "dry" systems, in wet systems the dominant convection mechanism is fluid driven. The dynamics are not then particularly sensitive to the grain-wall friction coefficient used [12].

Two methods of describing the fluid-grain interactions have been considered. The first model used is referred to as the simple Stokes drag (SD) model [30]. Here, a modified Stokes' drag force derived from the empirical bed equation of Ergun [25] is applied to each particle. The force is dependent on the particle size and its velocity relative to the container base. In this model the fluid is taken to follow the one-dimensional vertical motion of the container as it would do if no particles were present. This model does not allow two-dimensional fluid flow.

The second, principal, model is referred to as the Navier-Stokes (NS) model. In this model the fluid flow is reproduced using a modified version of the two-dimensional Navier-Stokes equations for the velocity and pressure fields. These equations include the fluid-grain interactions through a term involving the local mean variables of the grains, namely, the bed porosity and grain velocity. This interaction term has been derived from Ergun's bed equation [25]. The fluid momentum equation is discretised using the MAC scheme [31] and solved together with the fluid-grain continuity equations using the projection method [32]. Further details can be found elsewhere [12,19,33]. The two-dimensional treatment of the fluid flow is suitable for the box geometry used here and adequately describes fluid and granular convection. A model of this type has successfully been used to reproduce the Faraday tilting phenomena observed in vibrated granular beds [11].

6 Simulation results

We initially describe the simulation predictions for the behaviour of a mixture of 1500 bronze particles and 1500 glass particles immersed in the fluid with no magnetic field present. The mixture was vibrated at 20 Hz and $\Gamma = 2.0$. Under these vibratory conditions the mixture separates experimentally with the bronze grains on top. The SD model fails to adequately simulate the separation process. Since this model only reproduces the fluid damping without capturing the fluid-driven convection, the granular motion is confined to the vertical direction. Therefore, it is difficult for the grains of the different species to pass each other and reach the *bronze-on-top* state. The SD model can reproduce separation only at sufficiently high Γ and even then it will not capture the convection patterns observed experimentally. The use of this model indicates that the speed of separation and, in some cases, the development of a particular separation state is dependent upon granular convection and Faraday tilting. The need for a model which allows two-dimensional fluid flow has also been found for magnetic separation in air [18,19].

In Figure 8(a) the prediction of the NS model for the same system may be observed. Soon after vibration starts the bed breaks symmetry, thanks to a horizontal component in the fluid flow, and it develops a tilt. Fluid-driven–convection cells appear within the bed. This convective motion drives the grains around the bed, allowing the bronze grains to accumulate on top. As vibration continues, a bronze-rich region appears on top of the bed while a glass-rich region appears at the bottom. Within each of these two regions an independent convection cell is formed. The minority particles within each region are ejected from the region through convective motion allowing the mixture to reach almost pure separation with the bronze grains on top. The timescale for separation is about 1–2 minutes, in reasonably good agreement with the time observed experimentally. These results and similar results for other parameter values confirm the need to correctly treat the two-dimensional fluid motion in order to correctly reproduce the separation process.

In Figure 8(b) we show the predictions of the NS model for the behaviour of this mixture when a $B\mathrm{d}B/\mathrm{d}z = -55\,\mathrm{T}^2\mathrm{m}^{-1}$ is applied. Soon after vibration starts, the glass particles begin to accumulate on top. As vibration continues, the bed breaks symmetry. Two convection

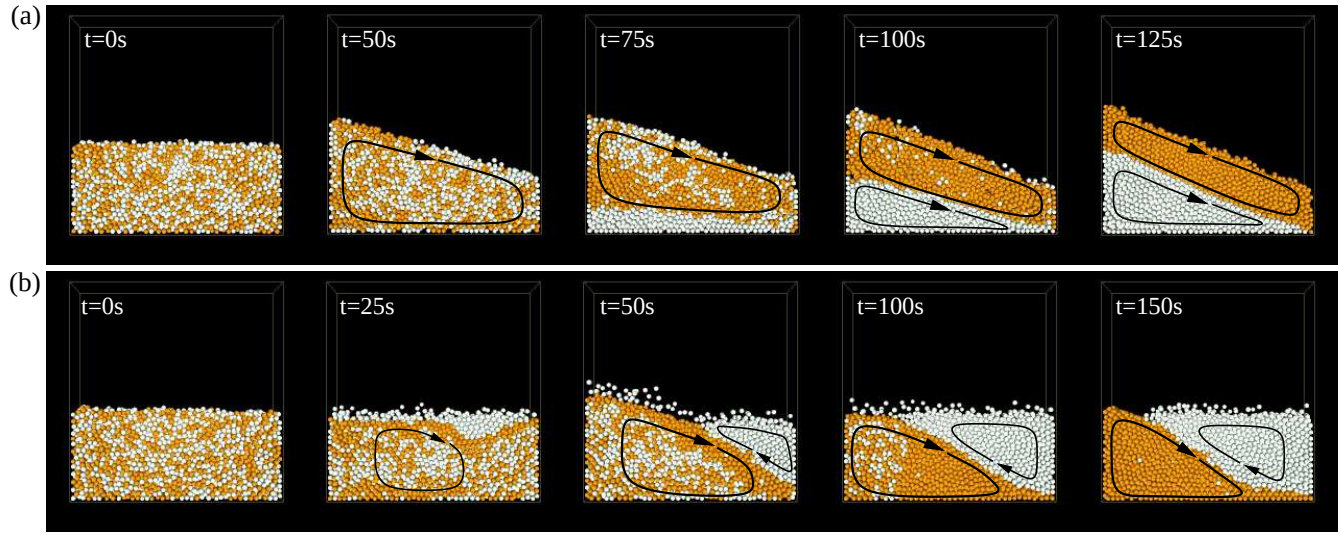

Fig. 8. Numerical predictions of the time development of the behaviour of a granular mixture of 1500 glass (white) and 1500 bronze (darker) spheres immersed in 1.5 M $MnCl_2$ when vibrated at 20 Hz and $\Gamma = 2.0$. (a) In zero magnetic field using the NS model, (b) with $B\mathrm{d}B/\mathrm{d}z = -55\,\mathrm{T^2m^{-1}}$ using the NS model.

cells circulating in the same direction can then be distinguished, one within the glass particles on top, the other in the bulk of the bed, rich in bronze particles. Further vibration leads to a complete separation with the vast majority of the glass grains on top of the bronze particles. The same sense of circulation within the separated regions causes apparent granular shearing at the interface between the separated layers. However, this granular convective motion does not cause mixing due to the formation of spatial gaps between the separated beds during flight, when the convective motion takes place. We will describe the dynamics of these gaps below.

In the experiments described above we have shown that different equilibrium states are achieved as $B\mathrm{d}B/\mathrm{d}z$ and Γ are changed. A characteristic convection pattern is associated with each equilibrium state. The NS model captures all the four equilibrium states found experimentally. While the order in which these states are observed is as in experiment, the simulated boundaries between configurations in the $(B\mathrm{d}B/\mathrm{d}z, \Gamma)$-plane are only in approximate agreement. The lack of exact quantitative agreement may be attributed to a number of factors including the use of an empirical bed equation derived for a static bed and the omission of lubrication effects during grain-grain impacts.

The simulations predict that the equilibrium states are also independent of the initial separation state of the mixture. As an example, for the specific mixture simulated here, the NS model predicts a *partially mixed* state at $\Gamma = 2.0$ and for $B\mathrm{d}B/\mathrm{d}z$ going from -30 to $-45\,\mathrm{T^2m^{-1}}$ as is shown in Figure 9(a). At that Γ the NS model predicts the transition to the *glass-on-top* state which is close to the experimental observations. *Sandwich* states are also predicted by the NS model. Figure 9(b) shows the sandwich state obtained at $B\mathrm{d}B/\mathrm{d}z = -50\,\mathrm{T^2m^{-1}}$ and $\Gamma = 2.8$. Because the NS model reproduces very many features of the experiments, we can use the model to gain insight into the detailed mechanics of the separation process.

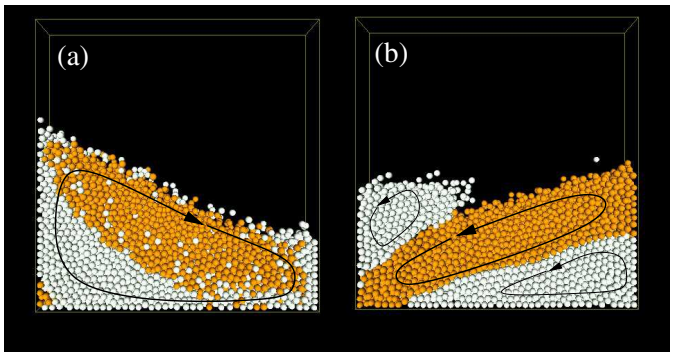

Fig. 9. A *partially mixed* state (a) and a *sandwich* state (b) found in simulations using the NS model. The vibratory and magnetic conditions were: (a) $B\mathrm{d}B/\mathrm{d}z = -40\,\mathrm{T^2m^{-1}}$ and $\Gamma = 2.0$; (b) $B\mathrm{d}B/\mathrm{d}z = -50\,\mathrm{T^2m^{-1}}$ and $\Gamma = 2.8$. The granular convection is indicated schematically by the arrowed lines.

7 Discussion of bed dynamics

To clarify aspects of the separation mechanism we have *separately* simulated the behaviour of a single granular bed of 1500 particles for each species of the mixture. For each bed we have measured the height above the base of the container during vibration at a fixed value of $\Gamma = 2.0$, both when no magnetic force is present and when a $B\mathrm{d}B/\mathrm{d}z = -60\,\mathrm{T^2m^{-1}}$ is applied. The results are shown in Figure 10.

When no magnetic force is present both beds take off at the same phase angle of vibration $\sin^{-1}(1/\Gamma)$. However, the height reached by the glass bed and the time of flight is considerably less than that of the bronze bed. This is expected since the density of glass is considerably lower than the density of bronze and, thus, the motion of the glass bed is more influenced by the fluid damping than the motion of the bronze bed.

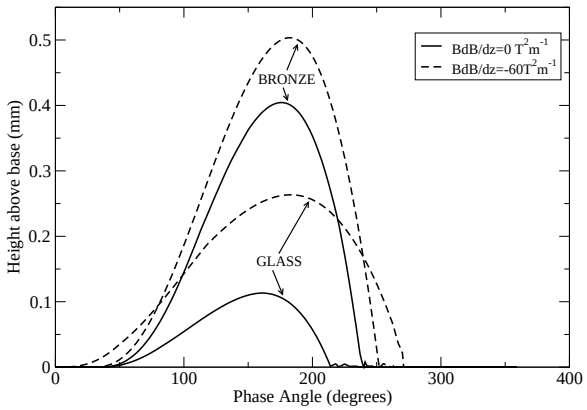

Fig. 10. Flight trajectories of a single glass bed and a single bronze bed vibrated at $\Gamma = 2.0$ and $f = 20\,\mathrm{Hz}$ when no magnetic force is present (solid line) and when a $B\mathrm{d}B/\mathrm{d}z = -60\,\mathrm{T^2m^{-1}}$ is applied (dashed line).

The difference between the motions of the individual beds when no magnetic force is present illustrates the basic principle of the VIFD separation of a mixture. In a mixture, the bronze grains accumulate on top thanks to their tendency to spend more time in flight during each cycle than the glass grains. The bronze particles are ratcheted upwards over many vibration cycles resulting in the *bronze-on-top* configuration. During flight, when the bed porosity is enhanced, an appreciable gap opens between the upper bronze and lower glass beds and granular convection occurs as a start-stop process during this period. It is this gap which allows for almost perfect separation [9]. Our simulations show that these results also represent the vertical behaviour of the separated beds of the *bronze-on-top* configuration even in the presence of Faraday tilting and the associated granular convection.

Figure 10 also shows the trajectories of the two beds when $B\mathrm{d}B/\mathrm{d}z = -60\,\mathrm{T^2m^{-1}}$ is applied. Since the glass grains have a smaller $\tilde{g}$ they take off earlier than the bronze grains. Although the maximum height reached by the glass bed is almost double than when no magnetic force is present, it is still lower than the maximum height achieved by the bronze particles. However, the glass grains now spend more time each cycle in flight than the bronze particles. Consequently, in a glass-bronze mixture vibrated under these conditions, it will now be the glass particles which accumulate on top. As we have shown above, $\Gamma = 2.0$, and $B\mathrm{d}B/\mathrm{d}z = -60\,\mathrm{T^2m^{-1}}$ are conditions under which a mixture is observed to separate into the *glass-on-top* state.

Finally, it is interesting to examine the dynamics of the beds in the separated state, in order to understand the partially mixed and the sandwich configurations. To do this we have studied, under two different field conditions, $B\mathrm{d}B/\mathrm{d}z$: $-60\,\mathrm{T^2m^{-1}}$ and $-40\,\mathrm{T^2m^{-1}}$, the dynamics of a mixture initially forced into a *glass-on-top* state in which the layers are *untilted*. The mixture was vibrated at 20 Hz and $\Gamma = 2.0$. Under these vibratory conditions the experimental equilibrium configuration observed at $B\mathrm{d}B/\mathrm{d}z = -60\,\mathrm{T^2m^{-1}}$ is *glass on top* and at $B\mathrm{d}B/\mathrm{d}z = -40\,\mathrm{T^2m^{-1}}$ a *partially mixed* configuration is observed. After vibration has been applied but before the grains experienced any modification from the initial *glass-on-top* state, we determined the vertical positions of the centres of mass of the bronze and glass particles, Z_B and Z_G, respectively, Figure 11(a). This figure shows a schematic representation of the initial state of the mixture.

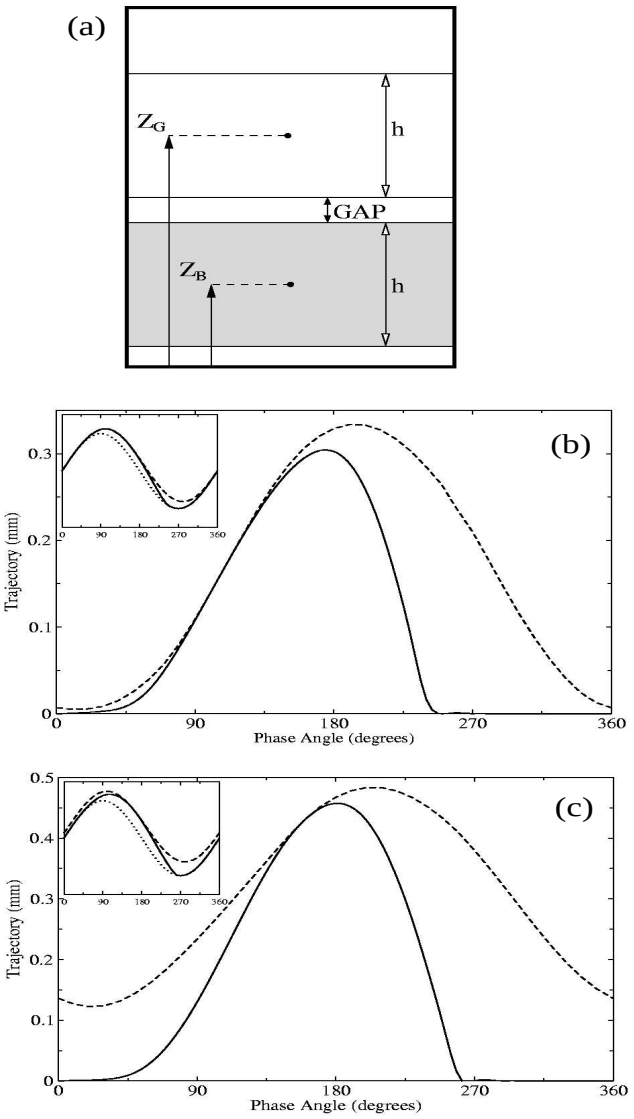

Fig. 11. Schematic representation of the initial configuration of the bed. A glass bed of height h flies above a bronze bed (light grey) of the same height. Panel (b) shows the glass (dashed) and bronze bed (solid) trajectories with respect to the vibrating container during one cycle of vibration when $B\mathrm{d}B/\mathrm{d}z = -40\,\mathrm{T^2m^{-1}}$. Panel (c) shows the trajectories of both beds when $B\mathrm{d}B/\mathrm{d}z = -60\,\mathrm{T^2m^{-1}}$. The small graphs on the top left corner of panels (b) and (c) show the exaggerated trajectories of the beds with respect the static frame of the laboratory, the dotted lines represents the oscillatory motion of the container.

Since we used the same number of glass and bronze spheres and in flight the bed porosity is never far from its static value, the beds of both components had the same mean bed depth h. To obtain the flight trajectory of the bronze bed $h/2$ was subtracted from Z_B while $3h/2$ was subtracted from Z_G to obtain the flight trajectory of the glass bed. Z_B and Z_G were measured every 10° of the phase angle of vibration ωt, over 3 cycles of vibration and then averaged. We have only averaged a small number of cycles to avoid the effects of the developing Faraday tilting.

The results for $B\mathrm{d}B/\mathrm{d}z = -40\,\mathrm{T^2m^{-1}}$ and $B\mathrm{d}B/\mathrm{d}z = -60\,\mathrm{T^2m^{-1}}$ are respectively shown in Figures 11(b) and (c). In both diagrams the solid line represents the trajectory of the bronze bed above the container base, while the dashed line shows the trajectory of the glass bed above the bronze bed. Both trajectories correspond to the motion of the beds in the frame of reference of the oscillating container. The small diagrams in the top left corner of each graph represent the bed trajectories in the static frame of reference of the laboratory.

With a $B\mathrm{d}B/\mathrm{d}z$ of $-40\,\mathrm{T^2m^{-1}}$, the glass and the bronze bed move together during almost all the first half of the vibratory cycle, as Figure 11(b) shows. Later, viewed from the frame of reference of the container, the bronze bed moves downwards faster than the glass bed due to its higher $\tilde{g}$ and a small gap opens between the beds. If the vibrations are allowed to continue the beds tilt and the mixture reaches the *partially mixed* configuration previously shown in Figure 9(a). The simulations show that during the period early in flight when the bronze and glass beds are dilated and mobile, they are in contact and move together at the very rough interface, thus maintaining the single convection cell which is found in this configuration.

When $B\mathrm{d}B/\mathrm{d}z$ is $-60\,\mathrm{T^2m^{-1}}$, the gap between the beds remains open for most of the vibratory cycle, as Figure 11(c) shows. In fact, the beds only touch each other briefly at around a phase angle of 170°. This happens because at this level of magnetic buoyancy the flight of the glass bed extends from one cycle of vibration to the next. Soon after the next vibratory cycle begins the bronze grains are thrown upwards and collide again with the glass grains as both species move downwards, repeating the cyclic motion. If vibration is allowed to continue the beds tilt but the configuration remains *glass on top*. The vertical motions described above are little changed. Because the gap between the glass and the bronze remains open during most of the vibratory cycle, the convective motion of the bronze grains cannot influence the glass particles, which remain on top as vibration continues.

Finally the stability of the *sandwich* configuration depends upon features both of the *bronze-on-top* state and of the *glass-on-top* state. The central bronze layer and the lower glass layer can maintain separated convection cells and do not mix since the bronze is thrown higher than the glass and there is an appreciable gap between them while they are in flight and dilated. The upper glass layer *bounces* lightly upon the bronze layer as in the *glass-on-top* configuration. Again separate convection cells may be maintained due to the gap between them.

8 Conclusions

We have studied the behaviour of mixtures of glass and bronze grains when they are vertically vibrated within a paramagnetic fluid, examining the balance between the VIFD and magneto-Archimedean buoyancy separation mechanisms. For containers wide enough to allow free convection, four distinct separation configurations have been identified each with their own characteristic pattern of convection. It has been argued that the range of magnetic and vibratory conditions for the *bronze-on-top* and *glass-on-top* configurations may be understood qualitatively by considering the balance between inertia, fluid-drag and magnetic buoyancy forces. The dependence of the separation boundaries on the magnetic susceptibility may also be qualitatively understood in this way. Quantitative details of the bed dynamics and the mechanisms behind the boundary between *partially mixed* and *sandwich* states have been successfully investigated through a numerical simulation method based on the Navier Stokes equations, a method which allows for two-dimensional fluid flow. It has been shown that these simulations predict the four states which we have observed and enable an understanding of their stability based on the gaps which open up between the beds during flight. With this understanding, magneto-Archimedean buoyancy is shown to be a useful and flexible method of controlling the separation of granular mixtures, which may then be based on either differences in density or differences in ρd^2.

We are grateful to the workshop staff of the School of Physics and Astronomy for their skills and enthusiasm and to K.A. Benedict and R.M. Bowley for helpful discussions. We thank R. Milburn for his invaluable assistance with the simulations. This work was supported by Research Councils UK through Basic Technology Grant No. GR/S83005/01.

References

1. B.A. Wills, *Mineral Processing Technology*, 6th ed. (Butterworth and Heinmann, London, 1997).
2. A. Kudrolli, Rep. Prog. Phys. **63**, 209 (2004).
3. N. Burtally, P.J. King, M.R. Swift, Science **295**, 1877 (2002).
4. N. Burtally, P.J. King, M.R. Swift, M.C. Leaper, Granular Matter **5**, 57 (2003).
5. C. Zeilstra, M.A. van der Hoef, J.A.M. Kuipers, Phys. Rev. E **74**, 029901 (2006).
6. A.B. Basset, Philos. Trans. R. Soc. London, Ser. A **179**, 43 (1888).
7. L.D. Landau, E.M. Lifschitz, *Fluid Mechanics* (Pergammon, Oxford, 1959).
8. C.F.M. Coimbra, R.H. Rangel, Am. Inst. Aeronaut. Astronaut. J. **39**, 1673 (2001).
9. M.C. Leaper, A.J. Smith, M.R. Swift, P.J. King, Granular Matter **7**, 57 (2005).
10. M. Faraday, Philos. Trans. R. Soc. **52**, 299 (1831).
11. R. Milburn, M. Naylor, A.J. Smith, M.C. Leaper, K. Good, M.R. Swift, P.J. King, Phys. Rev. E **71**, 011308 (2005).

12. R. Milburn, M.R. Swift, P.J. King, Powders Grains **2**, 1029 (2005).
13. A.T. Catherall, P. López-Alcaraz, P. Sanchez, M.R. Swift, P.J. King, Phys. Rev. E **71**, 021303 (2005).
14. See, for example, R.E. Rosensweig, *Ferrohydrodynamics* (Dover, 1998).
15. W. Braunbeck, Z. Phys. **112**, 764 (1939).
16. W. Braunbeck, Z. Phys. **112**, 753 (1939).
17. M. Berry, A. Geim, Eur. J. Phys. **18**, 307 (1997).
18. A.T. Catherall, M.R. Swift, P.J. King, Powders Grains **2**, 1025 (2005).
19. A.T. Catherall, R.J. Milburn, M.R. Swift, P.J. King, Granular Matter **9**, 169 (2007).
20. Y. Ikezoe, N. Hirota, K. Kitazawa, Nature **393**, 749 (1998).
21. Y. Ikezoe, T. Kaihatsu, S. Sakae, H. Uetake, N. Hirota, K. Kitazawa, Energy Conserv. Manage. **43**, 417 (2002).
22. A.T. Catherall, P.J. King, L. Leaves, S.R. Booth, Nature **422**, 579 (2003).
23. A.T. Catherall, P. López-Alcaraz, K.A. Bendict, L. Eaves, P.J. King, New J. Phys. **7**, 118 (2005).
24. A.T. Catherall, Doctoral Thesis, University of Nottingham (2005).
25. S. Ergun, Chem. Eng. Prog., **48**, 89 (1952).
26. P. Cundall, O. Strack, Geotechnique **29**, 47 (1979).
27. P. Gondret, M. Lance, L. Petit, Phys. Fluids **14**, 643 (2002).
28. M. Allen, D. Tildesley, *Computer Simulation of Liquids* (Oxford University Press, 2000).
29. R.G. Gutman, Trans. Inst. Chem. Eng. **54**, 174 (1976).
30. P. Biswas, P. Sanchez, M.R. Swift, P.J. King, Phys. Rev. E **68**, 050301 (2003).
31. F.H. Harlow, J.E. Welch, Phys. Fluids **8**, 2182 (1965).
32. A.J. Chorin, Math. Comput. **22**, 745 (1968).
33. R.J. Milburn, Doctoral Thesis, University of Nottingham (2006).